

LPV Model Order Reduction by Parameter-Varying Oblique Projection

Julian Theis, Peter Seiler, and Herbert Werner

Abstract—A method to reduce the dynamic order of linear parameter-varying (LPV) systems in grid representation is developed in this paper. It consists of an oblique projection and is novel in its use of a parameter-varying nullspace to define the direction of this projection. Parameter-varying state transformations in general lead to parameter rate dependence in the model. The proposed projection avoids this dependence and maintains a consistent state space basis for the reduced-order system. This extension of the projection framework lends itself very naturally to balanced truncation and related approaches that employ Gramian-based information to quantify the importance of subspaces. The proposed method is first compared to LPV balancing and truncation on a numerical example and then used to approximate two LPV systems: the longitudinal dynamics model of an aeroservoelastic unmanned aerial vehicle and the far wake model of a wind turbine.

Index Terms—Linear parameter-varying (LPV) systems, model order reduction.

I. INTRODUCTION

A METHOD to reduce the number of state variables of linear parameter-varying (LPV) systems in grid representation is developed in this paper. LPV models are particularly useful for the design and analysis of gain-scheduled controllers due to the availability of powerful synthesis techniques and computational tools [1], [2]. Both analysis and synthesis require the solution of linear matrix inequalities (LMIs). The required computation for this solution grows rapidly with increasing state dimension and hence limits applicability to models with relatively few state variables. With current tools, models with an order of about 50 state variables are tractable. For many physically motivated models, directly obtaining models with such a low order is not easy. For instance, structural mechanics models are often obtained from finite element analysis with a dense grid of nodes and hence these models have a large number of state variables. Similarly,

unsteady aerodynamic models often have several thousands of state variables. The method proposed in this paper can be used to obtain low-order models that can be used for LPV analysis and synthesis. It thus helps to increase the applicability of LPV control techniques to models that are otherwise out of the scope.

LPV model order reduction was first addressed in [3] and [4] by generalizing the concept of balancing and truncation [5]. Balancing and truncation consist of a state space coordinate transformation followed by removing state variables that are considered negligible in the new coordinates. The procedure requires the solution of LMIs to obtain generalized Gramians. Hence, this approach suffers from the same computational limitations as LPV analysis and synthesis problems. In addition, LPV balancing, in general, involves parameter-varying transformations. Parameter-varying transformations acknowledge the parameter dependence of the dynamic system, but introduce additional rate terms. In order to avoid this rate dependence, possibly conservative constant transformations have to be used. Model order reduction by parameter-varying oblique projection takes a middle ground and uses a partially parameter-varying projection. It turns out that this projection has a clear interpretation in terms of a varying test space in the Petrov-Galerkin approximation of dynamic systems. The main technical contribution is thus a possibility to use a partially parameter-varying projection without the introduction of additional rate dependence. This extension of the projection framework relates very naturally to balanced truncation and related approaches that employ Gramian-based information to quantify the importance of subspaces for model order reduction.

Several other approaches have been proposed for LPV model order reduction, which use linear time-invariant (LTI) techniques for frozen-parameter models, and then seek to interpolate the reduced-order models for time-varying parameters [6]–[10]. These approaches in general struggle with maintaining a consistent state space basis for the reduced-order system. This problem is avoided by using the parameter-varying oblique projection proposed in this paper. In recent years, the problem of *parametric model reduction* has also received considerable attention [11]–[13]. Parametric model reduction considers only constant parameter values and the goal is to approximate a family of parameterized LTI models. This differs substantially from the *LPV model order reduction* problem studied in this paper, which considers time-varying parameter values and whose goal is to approximate an LPV model. The proposed method nevertheless includes parametric

Manuscript received October 12, 2016; revised January 30, 2017; accepted February 28, 2017. Manuscript received in final form March 14, 2017. This work was supported by NASA entitled “Lightweight Adaptive Aeroelastic Wing for Enhanced Performance Across the Flight Envelope,” under Grant NRA NNX14AL36A. Recommended by Associate Editor S. Tarbouriech. (Corresponding author: Julian Theis.)

J. Theis and H. Werner are with the Institute of Control Systems, Hamburg University of Technology, 21073 Hamburg, Germany (e-mail: julian.theis@tuhh.de; h.werner@tuhh.de).

P. Seiler is with the Department of Aerospace Engineering and Mechanics, University of Minnesota, Minneapolis, MN 55414 USA (e-mail: seile017@umn.edu).

Color versions of one or more of the figures in this paper are available online at <http://ieeexplore.ieee.org>.

Digital Object Identifier 10.1109/TCST.2017.2692744

models as a special case of LPV systems, and hence can also be applied to this problem class.

This paper describes parameter-varying projection as a versatile order reduction method for LPV systems. It demonstrates the effectiveness of the approach, first introduced in [14], on two detailed application examples. The first example is the high-fidelity model of the longitudinal dynamics of a small unmanned aeroservoelastic aircraft, where the number of state variables is reduced from 48 to 12. The second example is a model for unsteady aerodynamics behind a wind turbine, where a reduction from 20 502 to 6 state variables is achieved.

II. BACKGROUND

LPV systems are dynamic systems whose state space representation involves continuous matrix functions of a time-varying parameter vector $\rho(t) \in \mathbb{R}^{n_\rho}$ that is not known in advance but measurable at each time instant. This makes LPV systems different from linear time-varying (LTV) systems, where time dependence is exactly known. In fact, LPV systems can be seen to encompass a family of LTV systems. For any specific parameter trajectory within the set of admissible trajectories, the LPV system becomes an LTV system. Similarly, for a fixed parameter value, the LPV system becomes an LTI system. Based on physical considerations, admissible parameter trajectories are confined to a compact set $\mathcal{P} \subset \mathbb{R}^{n_\rho}$ that is commonly approximated by a finite-dimensional subset $\{\rho_k\}_{k=1}^{n_g} \subset \mathcal{P}$, called a grid. Such a representation naturally arises, e.g., if a nonlinear system is linearized at multiple operating conditions. It is also the most general way of representing an LPV system and requires no further assumptions on the form of parameter dependence other than possibly restricting the admissible parameter variation by rate bounds $|\dot{\rho}_i| < v_i$, $i = 1, \dots, n_\rho$ [15]. The state space representation for an LPV system in terms of state vector $x(t) \in \mathbb{R}^{n_x}$, input vector $u(t) \in \mathbb{R}^{n_u}$, and output vector $y(t) \in \mathbb{R}^{n_y}$ is

$$\begin{aligned}\dot{x}(t) &= A(\rho(t))x(t) + B(\rho(t))u(t) \\ y(t) &= C(\rho(t))x(t) + D(\rho(t))u(t).\end{aligned}\quad (1)$$

The problem of LPV model order reduction consists of finding an approximation for the dynamic system (1) as

$$\begin{aligned}\dot{z}(t) &= A_{\text{red}}(\rho(t))z(t) + B_{\text{red}}(\rho(t))u(t) \\ y(t) &= C_{\text{red}}(\rho(t))z(t) + D_{\text{red}}(\rho(t))u(t).\end{aligned}\quad (2)$$

A reduced state vector $z(t) \in \mathbb{R}^{n_z}$ should be of much lower dimension than $x(t) \in \mathbb{R}^{n_x}$, while the input-output behavior from u to y should be as similar as possible to that of the original model. Further, stability of the original model should be preserved in the reduced-order model.

In the remainder of this paper, time dependence is dropped and parameter dependence is denoted by the subscript ρ , i.e., $A_\rho := A(\rho(t))$.

A. Oblique Projection and Model Order Reduction

An oblique projection is a linear operation defined by a matrix $\Pi = V(W^T V)^{-1}W^T$ with $V \in \mathbb{R}^{n_x \times n_z}$, $W \in \mathbb{R}^{n_x \times n_z}$, and $\text{rank}(W^T V) = n_z$. A projection is idempotent, i.e.,

$\Pi = \Pi^2$, and it is completely characterized by its range space $\text{span}(\Pi) = \text{span}(V)$ and its nullspace $\ker(\Pi) = \text{span}(\Pi^T)^\perp = \text{span}(W)^\perp$. This fact is easy to prove by replacing V and W with their respective thin QR-factorizations. A vector space is said to be projected by Π along the orthogonal complement of the subspace spanned by the columns of W and onto a subspace spanned by the columns of V . The projection thus restricts the vector space \mathbb{R}^{n_x} to a lower dimensional subspace $\text{span}(V) \subset \mathbb{R}^{n_x}$. Reference [16, Corollary 2.1] shows that any projection can be parameterized by V and a symmetric positive definite matrix $S \in \mathbb{R}^{n_x \times n_x}$ as

$$\Pi = V \underbrace{(V^T S V)^{-1} V^T S}_{W^T}. \quad (3)$$

Any W constructed in this way is biorthogonal to V , i.e., $W^T V = I_{n_z}$. Thus, from this point on, biorthogonality of V and W is assumed without loss of generality.

Given V and W with $W^T V = I_{n_z}$ and a point $x \in \mathbb{R}^{n_x}$, the projection of x lies in the span of V and hence can be written as Vz with some coefficient vector $z \in \mathbb{R}^{n_z}$. The component of x that is eliminated by the projection is in the nullspace of Π and hence orthogonal to W . This can be stated as $W^T(x - Vz) = 0$. The projection Πx can thus be seen as an approximation to x in $\text{span}(V)$ with zero error within $\text{span}(W)$. The subspace $\text{span}(V)$ is consequently termed *basis space* of the approximation and $\text{span}(W)$ is called *test space*.

LPV model order reduction requires the approximation of a dynamic system given by a differential equation, rather than an approximation for a single point in the state space. The goal is thus to find an approximate solution $x_{\text{approx}} = Vz$ to the state equation in (1)

$$\underbrace{\dot{x}_{\text{approx}}}_{V\dot{z}} \approx A_\rho \underbrace{x_{\text{approx}}}_{Vz} + B_\rho u. \quad (4)$$

From the previous discussion, Vz is uniquely determined by $z = W^T x$ for given V , W , and x . Hence, the right-hand side of (4) is known for a given state x and input u . A solution for the n_z -dimensional vector \dot{z} , however, requires the n_x equations imposed by (4) to be satisfied. Consequently, no \dot{z} exists, in general, that exactly satisfies (4). The residual of the approximation is

$$r := V\dot{z} - (A_\rho Vz + B_\rho u). \quad (5)$$

If \dot{z} is now selected such that the residual (5) is restricted to be orthogonal to the test space $\text{span}(W)$, that is

$$W^T(V\dot{z} - (A_\rho Vz + B_\rho u)) = 0 \quad (6)$$

the procedure is known as *Petrov-Galerkin approximation* [17], [18]. The unique solution to (6) is

$$\dot{z} = W^T A_\rho V z + W^T B_\rho u. \quad (7)$$

The desired approximation is hence given by $x_{\text{approx}} = Vz$, where z is the solution to (7). Adding the output equation $y = C_\rho x_{\text{approx}} + D_\rho u$ to (7) then yields the reduced-order

model

$$\begin{aligned} \dot{z} &= \overbrace{W^T A_\rho V}^{A_{\text{red},\rho}} z + \overbrace{W^T B_\rho}^{B_{\text{red},\rho}} u \\ y &= \underbrace{C_\rho V}_{C_{\text{red},\rho}} z + D_\rho u. \end{aligned} \quad (8)$$

B. State-of-the-Art LPV Balancing and Truncation

Section II-A shows how a reduced-order model is obtained by oblique projection for a given basis space and test space. It does not, however, provide any statements about the choice of these spaces. The state-of-the-art method of calculating a reduced-order LPV model was proposed in [3] and [4] by generalizing the concept of balancing and truncation from [5]. It calculates a desirable basis space and test space for the projection (8) from a generalized controllability Gramian X_c and a generalized observability Gramian X_o . These Gramians are symmetric positive definite matrices that $\forall \rho \in \mathcal{P}$ satisfy the LMIs

$$A_\rho X_c + X_c A_\rho^T + B_\rho B_\rho^T \prec 0 \quad (9a)$$

$$A_\rho^T X_o + X_o A_\rho + C_\rho^T C_\rho \prec 0. \quad (9b)$$

The \prec in (9) denotes negative definiteness of the symmetric matrix function on the left-hand side. Given a point x_0 in the state space, the minimum energy required to steer the system from $x = 0$ to $x = x_0$ is lower bounded by $\epsilon_c = x_0^T X_c^{-1} x_0$. Further, $\epsilon_o = x_0^T X_o x_0$ is an upper bound on the energy of the free response to the initial condition x_0 [4]. The ratio ϵ_o/ϵ_c thus indicates how much a state variable is affected by the input and how much it affects the output.

It is possible to perform a balancing transformation

$$\begin{bmatrix} x_1 \\ x_2 \end{bmatrix} = T x$$

so that $T X_c T^T = (T^{-1})^T X_o T^{-1} = \Sigma^{1/2}$, where the matrix Σ is diagonal and contains the eigenvalues of the product $X_c X_o$ ordered by decreasing magnitude along its diagonal. Since these values are exactly the ratios ϵ_o/ϵ_c for each state variable in the new coordinates, Σ has a similar interpretation as the matrix of Hankel singular values for LTI systems [5]. It is however nonunique and the common strategy is to calculate generalized Gramians from the (nonconvex) optimization problem

$$\min_{X_c, X_o} \text{trace}(X_c X_o) \text{ s.t. LMI (9)} \quad (10)$$

in order to increase the number of small singular values [4].

The balancing transformation can be used to first partition the state space representation such that $z := x_1$ contains the state variables with large singular values and x_2 those with small singular values. In the second step, x_2 is then removed from the state vector by truncation, so that the system (2) is obtained. Alternatively, these two steps can be combined into one single oblique projection by directly considering the Gramians to define the range space and null space of such a projection. A popular way of doing this is known as the *square root algorithm* [19]. It requires the

lower Cholesky factorizations $X_o = L_o L_o^T$ and $X_c = L_c L_c^T$, as well as the singular value decomposition (SVD) of the product

$$L_c^T L_o = [U_1 \ U_2] \begin{bmatrix} \Sigma_1 & \\ & \Sigma_2 \end{bmatrix} [N_1 \ N_2]^T. \quad (11)$$

The singular values are ordered by descending magnitude, such that the diagonal matrix Σ_1 contains the largest n_z singular values. The orthogonal matrices $[U_1 \ U_2]$ and $[N_1 \ N_2]$ contain the corresponding left and right singular vectors.¹ The basis space is then $\text{span}(L_c U_1)$ and the test space is $\text{span}(L_o N_1)$ (see [18]–[20] for details.) The corresponding projection is

$$\Pi_{\text{bal}} = \underbrace{L_c U_1}_{V} \Sigma_1^{-1/2} \underbrace{\Sigma_1^{-1/2} N_1^T L_o^T}_{W^T}. \quad (12)$$

The reduced-order model is guaranteed to be stable and satisfies an error-bound in the induced L_2 -norm of twice the sum of the truncated singular values [4]. It is further possible to augment the full-order system with stable minimum-phase weighting filters in order to emphasize a certain frequency range, completely analog to the approach first introduced in [21] for LTI systems.

C. Limitations of the State-of-the-Art Method

Solutions to (9) exist only for quadratically stable LPV systems, as both (9a) and (9b) imply the existence of a symmetric positive definite matrix X that $\forall \rho \in \mathcal{P}$ satisfies $A_\rho^T X + X A_\rho \prec 0$ and hence the existence of a parameter independent Lyapunov function $x^T X x$ [22]. Further, controllability and observability are necessary for the existence of positive definite generalized Gramians.

Even for quadratically stable LPV systems, restricting the search space to constant Gramians might decrease the quality of the approximation. As already stated in [3], it is possible to use parameter-varying generalized Gramians for balancing in order to enlarge the search space. This requires to find symmetric positive definite matrix functions $X_{c,\rho}$ and $X_{o,\rho}$ on the set \mathcal{P} that $\forall \rho \in \mathcal{P}$ satisfy the LMIs

$$-\frac{d}{dt} X_{c,\rho} + A_\rho X_{c,\rho} + X_{c,\rho} A_\rho^T + B_\rho B_\rho^T \prec 0 \quad (13a)$$

$$\frac{d}{dt} X_{o,\rho} + A_\rho^T X_{o,\rho} + X_{o,\rho} A_\rho + C_\rho^T C_\rho \prec 0. \quad (13b)$$

In this case, the derivative of the parameter vector ρ enters affinely through the time derivative of the generalized Gramians, i.e., $d/dt X_{c,\rho} = \sum_{i=1}^{n_\rho} \partial X_{c,\rho} / \partial \rho_i \dot{\rho}_i$. Consequently, the LMIs (13) need to be satisfied not only for all admissible parameter values but also for both the positive and negative maximum rates of variation $\pm v_i$ at each parameter value [1], [3]. The full-order model must still be stable, but not necessarily quadratically stable, in order to obtain solutions to (13). Besides several technical issues detailed in [3], it is possible to again construct a basis space and a test space using the square root method (12). In this case, both matrices V and W are parameter-varying, i.e., they should be denoted by V_ρ and W_ρ .

¹The notation N is chosen here to avoid confusion with the matrix V used to denote a basis for the range space of a projection.

Repeating the Petrov-Galerkin approximation of Section II-A, $\dot{x}_{\text{approx}} = d/dt(V_\rho z) = V_\rho \dot{z} + \sum_{i=1}^{n_\rho} \partial V_\rho / \partial \rho_i \dot{\rho}_i z$, so that the residual is

$$r := V_\rho \dot{z} + \sum_{i=1}^{n_\rho} \frac{\partial V_\rho}{\partial \rho_i} \dot{\rho}_i z - (A_\rho V_\rho z + B_\rho u). \quad (14)$$

The reduced-order LPV model obtained by enforcing the orthogonality constraint $W_\rho^T r = 0$ is thus

$$\begin{aligned} \dot{z} &= W_\rho^T \left(A_\rho V_\rho - \sum_{i=1}^{n_\rho} \frac{\partial V_\rho}{\partial \rho_i} \dot{\rho}_i z \right) z + W_\rho^T B_\rho u \\ y &= C_\rho V_\rho z + D_\rho u. \end{aligned} \quad (15)$$

Equation (15) explicitly depends on the parameter rate $\dot{\rho}$ in addition to the original parameter ρ . Properly retaining this dependence enlarges the parameter space and increases the complexity of the model.

The second severe limitation of the method is the computational effort required to solve the LMIs by numerical methods. Even for parameter independent generalized Gramians, the problem involves the (repeated) solution of two semidefinite programs, each with $n_{\text{dec}} = n_x(n_x + 1)/2$ decision variables and n_g constraints. Parameter-varying Gramians require $2^{n_\rho} n_g$ constraints and increase the number of decision variables by a factor equal to the number of basis functions selected for the Gramians [3]. Standard algorithms for solving semidefinite programs of the form (10) require a number of floating point operations that scales with n_{dec}^3 [23]. The problem thus scales on the order of n_x^6 , which shows that larger state dimensions quickly become restrictive. Currently, even the parameter independent solution is limited to systems with up to about 50 state variables.

D. Local Gramian Approximations

Remedies to avoid the computational complexity of the LMI solution usually make use of a “local” approximation, i.e., they evaluate the LPV system for a fixed parameter value and apply methods for LTI systems. For a frozen parameter $\rho \equiv \rho_k$, the solution of (10) simplifies to solving the two Lyapunov equations

$$A X_c + X_c A^T + B B^T = 0 \quad (16a)$$

$$A^T X_o + X_o A + C^T C = 0. \quad (16b)$$

This follows from the fact that $Y - X < 0$ for all X and Y that satisfy $A X - X A^T + B B^T < 0$ and $A Y - Y A^T + B B^T = 0$ [24, Proposition 4]. A parameter independent projection that balances the state space representation for $\rho \equiv \rho_k$ can be applied to an LPV system with the assumption that it is similar to the projection that would balance the state space representation over the whole parameter space. For some applications [25], this approach can be successfully applied. If the dynamics vary substantially over the parameter space, such a constant projection is usually insufficient. It is then tempting to calculate local approximations of the Gramians at various parameter values and to interpolate between grid points. This interpolation is guaranteed to be smooth for a sufficiently dense grid, since $X_{c,\rho}$ and $X_{o,\rho}$ that satisfy (13) are

continuous functions of ρ [3]. The problem of additional rate dependence nevertheless remains, as the interpolated Gramian approximations are necessarily parameter-varying and therefore result in a parameter-varying projection. In case of either of these local approximations, any stability guarantees and error bounds are lost, since the local solutions only satisfy the LMI constraints at single points in the domain and not necessarily anywhere else.

For large-scale systems with several thousands of state variables, even the Lyapunov equations (16) become intractable. In this case, iterative low-rank approximations of the solutions to (16) can be used [26]–[28]. Alternatively, empirical Gramian approximations can be constructed from impulse response data that are obtained from simulations of the full-order model [5], [18], [29], [30]. Such approximations scale almost linearly with the state dimension.

III. LPV MODEL ORDER REDUCTION BY PARAMETER-VARYING OBLIQUE PROJECTION

There are two key issues with the state-of-the-art method: 1) parameter-varying projections introduce additional rate dependence which in practice restricts the search space to parameter independent Gramians; and 2) the computational limitations associated with solving the LMIs in order to determine a basis space and a test space for the projection. The first problem motivates the introduction of a partially parameter-varying projection in Section III-A that avoids additional rate dependence while maintaining additional freedom over parameter independent projections. The second problem is addressed in Section III-B by calculating suitable spaces for approximate balancing of the LPV state space representation from the local approximations of Section II-D that are numerically well tractable. The proposed method, summarized in Section III-C, can thus be used in case the LMI solution fails, either due to an overly restricted search space or due to computational complexity.

A. Parameter-Varying Oblique Projections

It was shown in Section II-C that a parameter-varying projection leads to rate dependence in the reduced-order model. Specifically, this additional dependence is caused by the *parameter-varying basis* V_ρ , that is

$$\dot{x}_{\text{approx}} = \frac{d}{dt}(V_\rho z) = V_\rho \dot{z} + \sum_{i=1}^{n_\rho} \frac{\partial V_\rho}{\partial \rho_i} \dot{\rho}_i z. \quad (17)$$

Rate dependence does not, however, depend on the test space and hence on the matrix W_ρ . Consequently, it is avoided in the reduced-order model by restricting V to be constant, regardless of whether W_ρ is parameter-varying.

Such a projection is formulated in Proposition 1.

Proposition 1: Let $V \in \mathbb{R}^{n_x \times n_z}$ be a given constant matrix with $\text{rank}(V) = n_z < n_x$ and let $S_\rho: \mathbb{R}^{n_\rho} \mapsto \mathbb{R}^{n_x \times n_x}$ be a given symmetric positive definite matrix function. Then

$$\Pi_\rho = V \underbrace{(V^T S_\rho V)^{-1} V^T S_\rho}_{W_\rho^T} \quad (18)$$

is a parameter-varying oblique projection and the dynamic LPV system obtained by Petrov-Galerkin approximation with constant basis space $\text{span}(V)$ and parameter-varying test space $\text{span}(W_\rho)$ does not depend on the rate of parameter variation.

Proof: It is readily verified that $W_\rho^T V = I_{n_z} \forall \rho$ and that hence $\Pi_\rho = \Pi_\rho^2$ is an oblique projection. Further, since V is constant, the projected state space equations (15) simplify to

$$\begin{aligned} \dot{z} &= \overbrace{W_\rho^T A_\rho V}^{A_{\text{red},\rho}} z + \overbrace{W_\rho^T B_\rho}^{B_{\text{red},\rho}} u \\ y &= \underbrace{C_\rho V}_{C_{\text{red},\rho}} z + D_\rho u. \end{aligned} \quad \square \quad (19)$$

The range of the projection (18) in Proposition 1 is constant but the nullspace of the projection, i.e., its direction, varies across the parameter space. The results are the seemingly paradox relations $Vz \approx x$ and $z \approx W_\rho^T x$ that become clearer once the Petrov-Galerkin approximation

$$\dot{x}_{\text{approx}} = V W_\rho^T A_\rho x_{\text{approx}} + V W_\rho^T B_\rho u \quad (20)$$

is considered. It is not the approximate state vector, but its derivative that is calculated according to a parameter-varying condition described by W_ρ . Hence, the state update is performed depending on the current parameter value, while the approximate state vector itself always remains in $\text{span}(V)$. The latter is an immediate consequence of idempotency of the projection, i.e., regardless of ρ , $x_{\text{approx}} = V W_\rho^T x_{\text{approx}}$.

The benefit of the projection in Proposition 1 over an arbitrary parameter-varying projection is that it avoids rate dependence in the reduced-order model. It still has additional freedom in constructing a reduced-order model compared to a completely parameter independent projection. This additional freedom is the choice of a parameter-varying nullspace, i.e., the Petrov-Galerkin condition (6) can be changed over the parameter-space. As an important consequence, the reduction in Proposition 1 can no longer be represented as a transformation, precisely because a transformation has no nullspace. In fact, it directly follows that if V has full row rank, the projection (18) simply becomes I_{n_x} .

B. Basis and Test Space Construction

Recall from Section II that LPV balancing and truncation is a Petrov-Galerkin approximation, where the basis space and test space are determined from generalized Gramians. These Gramians may be parameter dependent and their calculation requires the LMI solutions (13), which become intractable for many systems even of moderate state dimension. Local approximations of the Gramians as described in Section II-D are much easier to calculate, but usually lead to parameter dependent projections with additional rate dependence in the reduced-order model. This section establishes a method to calculate a parameter independent basis space and a parameter-varying test space from local Gramian approximations in a geometrically optimal way. These spaces satisfy the constraints of Proposition 1 and can thus be used to approximate the projection (12) without additional rate dependence.

First, the projection (12) for balancing and truncation is reformulated in the following proposition.

Proposition 2: Let the controllability and observability Gramians $X_o = L_o L_o^T$ and $X_c = L_c L_c^T$, and the singular value decomposition (SVD) of the product $L_c^T L_o = [U_1 U_2] \begin{bmatrix} \Sigma_1 & \Sigma_2 \end{bmatrix} [N_1 N_2]^T$ be given. Let Q denote a basis for $\text{span}(L_c U_1)$. A projection that achieves balancing and truncation is

$$\Pi_{\text{bal}} = Q(Q^T X_o Q)^{-1} Q^T X_o. \quad (21)$$

Proof: Let QR denote the thin QR-factorization of $L_c U_1$. Replacing Q by $L_c U_1 R^{-1}$ and X_o by $L_o L_o^T$ in (21) yields

$$\Pi_{\text{bal}} = L_c U_1 (U_1^T L_c^T L_o L_o^T L_c U_1)^{-1} U_1^T L_c^T L_o L_o^T.$$

It follows from the given SVD that $U_1^T L_c^T L_o = \Sigma_1 N_1^T$. Substitution of this expression results in

$$\Pi_{\text{bal}} = L_c U_1 (\Sigma_1 N_1^T N_1 \Sigma_1)^{-1} \Sigma_1 N_1^T L_o^T.$$

The equivalence to (12) is established by finally using the fact that $(\Sigma_1 N_1^T N_1 \Sigma_1)^{-1} \Sigma_1 = \Sigma_1^{-1}$. \square

Equating the form of an admissible parameter-varying oblique projection in Proposition 1 with the projection for balancing and truncation in Proposition 2, it is clear that the matrix X_o is allowed to be parameter dependent. Hence, a parameter dependent approximation for the generalized observability Gramian can directly be used. Nevertheless, a constant basis $Q \in \mathbb{R}^{n_x \times n_z}$ for the basis space is required to avoid rate dependence in the reduced-order model. In order to reproduce balancing and truncation, Q should be a basis for $\text{span}(L_{c,\rho} U_{1,\rho})$, where the span of the parameter-varying matrix refers to the parametrically varying vector space that is spanned by the matrix $L_{c,\rho_k} U_{1,\rho_k}$ for fixed values ρ_k . In general, this can only be achieved by a parameter-varying matrix Q_ρ , obtained, e.g., from a thin QR-factorization at each grid point. The remaining critical question is thus in what sense the constant subspace $\text{span}(Q)$ should approximate the parameter-varying subspace $\text{span}(Q_\rho)$. A practical approach for a geometrically optimal approximation over a grid of parameter values $\{\rho_k\}_{k=1}^{n_g}$ is given in the following proposition.

Proposition 3: Let $Q_\rho \in \mathbb{R}^{n_x \times n_z}$ with $Q_\rho^T Q_\rho = I_{n_z}$ be a given parameter dependent basis for the parameter-varying subspace $\text{span}(Q_\rho)$. Let further $[Q_{\rho_1} \cdots Q_{\rho_g}]^T$ denote the collection of function evaluations of Q_ρ on the grid of parameter values $\{\rho_k\}_{k=1}^{n_g}$. Let

$$[\bar{U}_1 \quad \bar{U}_2] \begin{bmatrix} \bar{\Sigma}_1 & \\ & \bar{\Sigma}_2 \end{bmatrix} [Q \quad Q_\perp]^T = \begin{bmatrix} Q_{\rho_1}^T \\ \vdots \\ Q_{\rho_g}^T \end{bmatrix} \quad (22)$$

be the SVD such that $\bar{\Sigma}_1$ contains the largest n_z singular values and $\bar{\Sigma}_2$ the remaining $n_x - n_z$ singular values. Then, $\text{span}(Q)$ is an optimal approximation for $\text{span}(Q_\rho)$ in the sense that its orthogonal complement Q_\perp minimizes

$$\min_{Q_\perp} \sum_{k=1}^{n_g} \|Q_{\rho_k}^T Q_\perp\|_F^2 \quad \text{s.t.} \quad Q_\perp^T Q_\perp = I_{n_x - n_z}. \quad (23)$$

Algorithm 1 Parameter-Varying Oblique Projection for Approximating Balanced Truncation

Input: LPV system $\{A_{\rho_k}, B_{\rho_k}, C_{\rho_k}, D_{\rho_k}\}_{k=1}^{n_g}$ and desired order n_z

Output: LPV system $\{A_{\text{red},\rho_k}, B_{\text{red},\rho_k}, C_{\text{red},\rho_k}, D_{\text{red},\rho_k}\}_{k=1}^{n_g}$

```

for  $k = 1$  to  $n_g$  do
   $L_{c,\rho_k} \leftarrow \text{lyapchol}(A_{\rho_k}, B_{\rho_k})^T$ 
   $L_{o,\rho_k} \leftarrow \text{lyapchol}(A_{\rho_k}^T, C_{\rho_k}^T)^T$ 
   $(U, \Sigma, \star) \leftarrow \text{svd}(L_{c,\rho_k}^T L_{o,\rho_k})$ 
   $(\bar{U}, \star, \star) \leftarrow \text{svd}(L_{c,\rho_k} U(1:n_x, 1:n_z))$ 
   $\bar{Q}(1:n_x, 1+n_z(k-1):n_z k) \leftarrow \bar{U}(1:n_x, 1:n_z)$ 
end for
 $(Q, \star, \star) \leftarrow \text{svd}(\bar{Q})$ 
 $V \leftarrow Q(1:n_x, 1:n_z)$ 
for  $k = 1$  to  $n_g$  do
   $(Q, R) \leftarrow \text{qr}(L_{o,\rho_k}^T V)$ 
   $W_{\rho_k} \leftarrow L_{o,\rho_k} Q (R^T)^{-1}$ 
   $A_{\text{red},\rho_k} \leftarrow W_{\rho_k}^T A_{\rho_k} V$ 
   $B_{\text{red},\rho_k} \leftarrow W_{\rho_k}^T B_{\rho_k}$ 
   $C_{\text{red},\rho_k} \leftarrow C_{\rho_k} V$ 
   $D_{\text{red},\rho_k} \leftarrow D_{\rho_k}$ 
end for

```

Proof: Since the equality $\|X\|_F^2 + \|Y\|_F^2 = \|\frac{X}{Y}\|_F^2$ holds for all matrices X and Y of compatible dimensions, (23) can be rewritten as

$$\min_{Q_{\perp}} \left\| \begin{bmatrix} Q_{\rho_1}^T \\ \vdots \\ Q_{\rho_{n_g}}^T \end{bmatrix} Q_{\perp} \right\|_F^2 \quad \text{s.t. } Q_{\perp}^T Q_{\perp} = I_{n_x - n_z}.$$

The minimizer is found from the SVD (22) and the optimal cost is $\|\bar{U}_2 \bar{\Sigma}_2\|_F^2$. \square

Proposition 3 states that a constant subspace $\text{span}(Q)$ is an optimal approximation for the parameter-varying subspace $\text{span}(Q_{\rho})$ if its orthogonal complement $\text{span}(Q_{\perp}) = \text{span}(Q)^{\perp}$ approximates the parameter-varying nullspace $\ker(Q_{\rho}^T)$. For a single grid point ρ_k , the matrix $Q_{\rho_k}^T Q_{\perp}$ is rank deficient and the optimal “approximation” that attains the exact minimum 0 is simply a basis for the nullspace $\ker(Q_{\rho_k}^T)$. Obviously, a constant basis cannot, in general, achieve a zero norm for multiple grid points at once if $\text{span}(Q_{\rho})$ is not constant. The cost function in (23) thus measures the average “nullspace violation” over all grid points.

This way of choosing a common basis space is, in fact, identical to the approach first proposed in the context of parametric model-order reduction in [13], but Proposition 3 establishes optimality and provides a clear interpretation of the procedure.

C. Implementation

The proposed model order reduction method is summarized as Algorithm 1. For convenience, Matlab notation is used, e.g., $Q(1:n_x, 1:n_z)$ denotes the first $n_x \times n_z$ elements of the matrix Q . A \star denotes quantities of no interest. The first step is to calculate the Cholesky factors $\{L_{c,\rho_k}\}_{k=1}^{n_g}$ and

$\{L_{o,\rho_k}\}_{k=1}^{n_g}$ of local Gramian approximations at each grid point ρ_k . While this is computationally the most challenging part of the reduction, efficient algorithms are readily available. It should be noted that the complete Gramians are never required and that thus Hammarling’s algorithm [31] (e.g., implemented in Matlab’s routine `lyapchol`) can be used to directly obtain the Cholesky factors from the Lyapunov equations (16). Alternatively, the standard Bartels-Stewart algorithm [32] followed by decomposition or an approximation as described in Section II-D can be used. The choice of n_z can be guided by the singular values obtained from the first SVD at each grid point, e.g., as $\text{trace}(\Sigma_2^2) < \epsilon$ or as $\text{trace}(\Sigma_1^2)/\text{trace}(\Sigma_2^2) < \epsilon$, where the threshold ϵ reflects a desired accuracy at the grid points.

The projection matrix W_{ρ} is calculated from a thin QR-factorization to facilitate the inversion in $W_{\rho} = X_{o,\rho} V (V^T X_{o,\rho} V)^{-1}$ [33]. The resulting state space representation of the reduced-order LPV model is valid on the same grid as the original model. Hence, the same interpolation method (commonly piecewise linear) can be used to recover models between grid points.

D. Stability Considerations and Limitations

Just like the LMI method, the proposed approach requires the full-order system to be stable, as well as observable and controllable for positive definite Gramian approximations to exist. If the subspaces are calculated from point-wise solutions, stability guarantees for the reduced-order model are lost, since the interpolated matrix functions do not necessarily satisfy the LMIs (13) due to the rate term. It is nevertheless possible to guarantee stability of the reduced-order model for “slowly” varying parameters when the Gramians are obtained as solutions to the Lyapunov equations (16). A result from [16] and the form of the projection for balancing and truncation given in Proposition 2 are invoked to show that all poles of the reduced-order system are in the left half-plane for parameters frozen at any grid point. Multiplying the Lyapunov equation (16b) for the full-order system from the left by Q^T and from the right by Q results in

$$Q^T A^T X_o Q + Q^T X_o A Q + Q^T C^T C Q = 0. \quad (24)$$

Using $A_{\text{red}} = (Q^T X_o Q)^{-1} Q^T X_o A Q$ and $C_{\text{red}} = C Q$, it can be shown that (24) is equivalent to

$$A_{\text{red}}^T (Q^T X_o Q) + (Q^T X_o Q) A_{\text{red}} + C_{\text{red}}^T C_{\text{red}} = 0. \quad (25)$$

Since X_o is symmetric positive definite, so is $Q^T X_o Q$ and consequently A_{red} has all its eigenvalues in the left half-plane. This property guarantees stability for sufficiently slow parameter variation [34]. When frequency-weighted Gramians or impulse responses are used to construct the projection, even this weaker stability property cannot be guaranteed anymore. It is however worth noting that an *a posteriori* stability test, that might also include rate bounds, can be performed by solving an LMI feasibility problem of the form $A_{\text{red},\rho}^T X + X_{\rho} A_{\text{red},\rho} - \sum_{i=1}^{n_{\rho}} \partial X_{\rho} / \partial \rho_i \dot{\rho}_i < 0$ [15]. Since this only involves the reduced-order model, the calculation is likely to be tractable, even if it is not for the full-order model.

As noted in Section III-A, the proposed method exploits the extra freedom in selecting a parameter-varying nullspace. It can therefore not be expressed as a transformation. As a consequence, the method is limited to projection-type model order reduction, i.e., it always truncates state variables that are not retained in the reduced-order model. Singular perturbation techniques, i.e., residualization of state variables that are to be removed, are therefore not applicable in conjunction with the proposed method.

The computational cost of the proposed algorithm is dominated by solving the two Lyapunov equations and calculating the SVD at all grid points. The number of floating point operations thus scales on the order of n_x^3 [32]. Ultimately, this limits the state dimension of problems that can be addressed by the proposed algorithm. However, this computational cost is significantly less than the cost of the formal LMI approach that scales on the order of n_x^6 [23].

IV. APPLICATION EXAMPLES

This section demonstrates the applicability and effectiveness of the proposed model order reduction method by means of three examples. First, a nonlinear mass-spring-damper system is used to compare the proposed approach with the formal LMI-based method, in terms of computational complexity and approximation error. The second example is a high-fidelity longitudinal dynamics model of an aeroservoelastic unmanned aerial vehicle. This multi-input-multi-output system is of moderate size, but poses a challenge due to the strong nonlinear dependence of its dynamic properties on the airspeed. Design of flight control systems for these types of aircraft requires accurate, yet low-order models. The final example is the far wake model of a wind turbine. Such large-scale models are relevant to study the aerodynamic interactions in a wind farm and to develop control strategies to maximize the overall power output of several turbines that are located close to each other. For all examples, a desktop PC with 3.4-GHz 8-core CPU and 8-GB RAM was used, running 64-bit Windows 7 and Matlab 2014b. It should be noted that the LMI-based method fails both on the second and third example. Whenever LPV simulations are performed, piecewise linear interpolation between neighboring grid points is used.

A. Nonlinear Mass-Spring-Damper System

The model is taken from [35] and represents the interconnection of 50 blocks with mass $m = 1$ kg, each connected both to their neighboring blocks and the initial system by a linear damper with damping constant $d = 1$ Ns/m and a nonlinear spring with stiffness $k(q) = k_1 + k_2 q^2$, where $k_1 = 0.5$ N/m and $k_2 = 1$ N/m³. An external force ρ and a controlled force u act on the 50th block. The equations of motion for the i th block in terms of its displacement q_i from the equilibrium are

$$m \ddot{q}_i = \begin{cases} -F_1 - F_{1,2}, & i = 1 \\ -F_i - F_{i,i-1} - F_{i,i+1}, & i = 2, \dots, 49 \\ -F_{50} - F_{50,49} + \rho + u & i = 50. \end{cases}$$

The force $F_{i,j} = d(\dot{q}_i - \dot{q}_j) + k_1(q_i - q_j) + k_2(q_i - q_j)^3$ is caused by the relative motion of neighboring blocks and

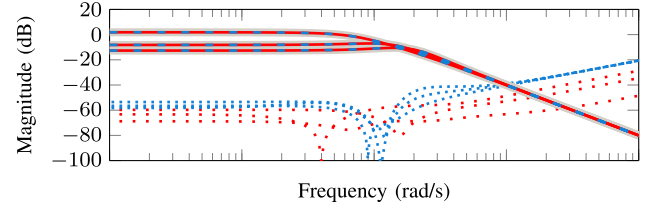


Fig. 1. Frequency response of mass-spring-damper system at frozen parameters $\rho = 0, 1, 2$ for original model (— 100 states), reduced-order model from LMI method (--- four states) and proposed algorithm (— four states), and relative error (LMI method --- and proposed algorithm —).

TABLE I
COMPARISON OF REDUCED-ORDER MASS-SPRING-DAMPER MODELS

	LPV Balancing	Proposed Algorithm
Computation Time [†]	9170 s	0.1 s
\mathcal{L}_2 -norm error bound	3.9e-03	12.1e-03
Local \mathcal{H}_∞ -norm error	2.2e-03	1.5e-03
Mean squared error	1.5e-03	1.5e-03

[†] on a 64 bit desktop PC with 3.4 GHz 8-core CPU and 8 GB RAM

$F_i = d \dot{q}_i + k(q_i) q_i$ is due to the connection with the initial system. The state vector is $[q_1, \dots, q_{50}, \dot{q}_1, \dots, \dot{q}_{50}]^T$ and the output is the displacement q_{50} . The parameter range is restricted to $\mathcal{P} = [0 \ 2]$ and the system is linearized on a grid $\{\rho_k\}_{k=1}^3 = \{0, 1, 2\}$. The function `lpvbalreal` of the LPVTools toolbox (v. 1.0) [2] is used to solve (9) for parameter independent generalized Gramians, which takes more than 2.5 hours. The proposed algorithm only takes 0.1 seconds and results in a very similar reduced-order model of order 4.

An upper bound $\bar{\gamma}$ on the error in the induced \mathcal{L}_2 -norm is calculated using the LPVTools function `lpvnorm`. This guarantees $\|e\|_2 < \bar{\gamma} \|u\|_2$ and certifies stability for arbitrary fast parameter variations. The formal approach yields a slightly better error bound $\bar{\gamma} = 3.9\text{e-}03$ compared with $\bar{\gamma} = 12.1\text{e-}03$ for the proposed method. Additionally, the maximum local \mathcal{H}_∞ -norm error $\underline{\gamma}$ at the grid points is calculated for frozen parameters. The proposed method results in $\underline{\gamma} = 1.5\text{e-}03$ compared with $\underline{\gamma} = 2.2\text{e-}03$ for the formal method and thus achieves a slightly better local error. The frequency responses are shown in Fig. 1. Time-domain responses are compared in Fig. 2. Both methods approximate the output equally well and result in an identical mean squared error of $1.5\text{e-}03$. Table I summarizes these results.

B. Aeroservoelastic Aircraft

A model of NASA's X56 Multi-Utility Technology Testbed aircraft is employed to demonstrate the use of the proposed method to obtain a control-oriented low-order model. The X56 is a research platform for control of highly flexible aircraft [36]. A schematic of the aircraft is shown in Fig. 3.

A high-fidelity model of the longitudinal dynamics is considered in this paper. It combines rigid-body flight dynamics from first principle modeling, structural dynamics from FEM modeling, and unsteady aerodynamics from CFD modeling [37]. The rigid body dynamics are described in the moving

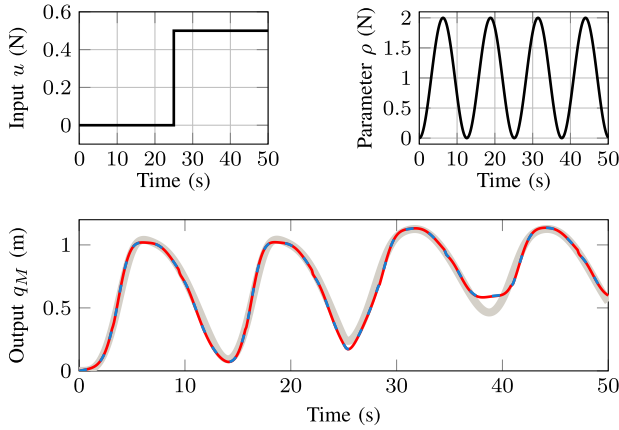


Fig. 2. Nonlinear simulation of mass-spring-damper system (— 100 states) and reduced-order model from LMI method (— four states) and proposed algorithm (— four states).

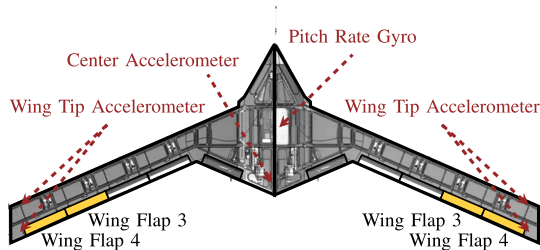


Fig. 3. X56A MUTT unmanned aerial vehicle.

body frame and represented by angle of attack α and pitch rate q . The flexible modal displacements are represented in terms of assumed mode shapes and generalized coordinates η . Unsteady aerodynamics are represented by state variables w and are related to the rigid and flexible degrees of freedom of the system. Specifically, every degree of freedom is coupled to a third order system that describes the unsteady aerodynamic forces caused by, and acting on, modal displacement. There are 8 structural modes (16 states), 2 rigid body states, and 30 aerodynamic states, which totals to 48 states. As inputs, symmetric deflection of the two outboard wing flap pairs (δ_3 and δ_4), highlighted in Fig. 3, is considered. The outputs are a pitch rate measurement q_{meas} and acceleration signal at the center body ($a_{z,\text{center}}$), as well as an averaged wing tip acceleration signal ($a_{z,\text{wing}}$) that combines measurements from the four sensors shown in Fig. 3.

The dynamics of the aircraft depend nonlinearly on the airspeed V_0 and the state space representation is of the form

$$\begin{aligned}\dot{x} &= A(V_0)x + B(V_0)\delta \\ y &= C(V_0)x + D(V_0)\delta\end{aligned}\quad (26)$$

with state vector $x = [w^T \mid \alpha \mid q \mid \dot{\eta}^T \mid \eta^T]^T$, output vector $y = [q_{\text{meas}} \ a_{z,\text{center}} \ a_{z,\text{wing}}]^T$, and input vector $\delta = [\delta_3 \ \delta_4]^T$. A grid representation with 12 uniformly spaced points is used to cover the domain $V_0 \in [30.6 \ 68]$ m/s. The aircraft is naturally stable in this domain but the damping ratio of the lowest-frequency aeroelastic mode decreases dramatically with higher airspeeds. Hence, the dynamics change rapidly.

For a control-oriented model, the available bandwidth of a control system provides an upper frequency limit on the

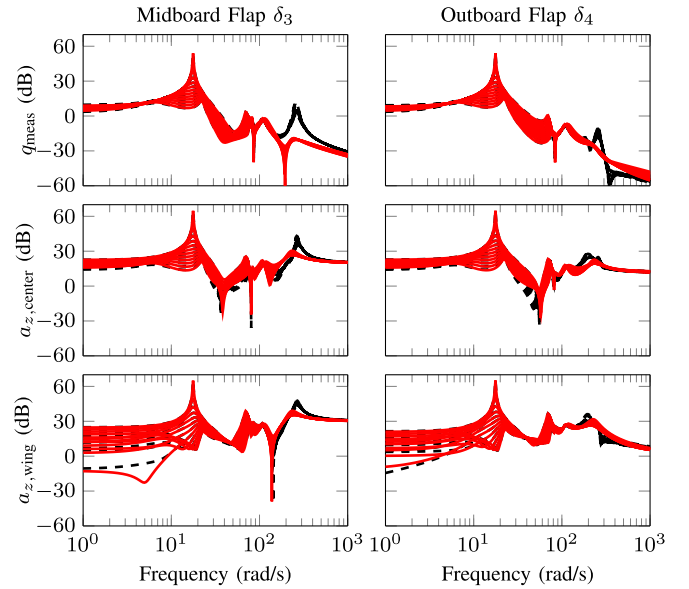


Fig. 4. X56A model: frequency responses at frozen parameter values for full-order (--- 48 states) and reduced-order model (— 12 states).

fidelity requirement. Frequency weighting is thus especially useful for this type of model. Fifth order butterworth filters with a cut-off frequency of 100 rad/s are selected for the present example. The augmented Lyapunov equations are solved using the Matlab routine `lyapchol` at each grid point.

The calculation takes only seconds and hence the order of the reduced model can be determined by trial and error. A 12th order model yields satisfactory results.

Fig. 4 shows the Bode magnitude plots of the full-order and the reduced-order model evaluated for frozen parameter values at the grid points. The reduced-order model agrees very well with the full-order model up to the specified frequency of 100 rad/s. The only noticeable discrepancy within the frequency range of interest is for the wingtip acceleration due to midboard flap deflection between 2 and 8 rad/s at 44 m/s airspeed. Fig. 5 shows the step response of both the full-order and the reduced-order model along a time-varying parameter trajectory. The trajectory covers the complete parameter space with a high rate of variation. The reduced-order model nevertheless approximates the response very well, also for the wing tip acceleration signal. The most prominent difference is visible in the high frequency transients right after application of the step input. The reduced-order model clearly omits these as a consequence of the frequency-weighted approximation. Fig. 6 shows the pole migration of both models over the parameter space with linear interpolation between grid points. The plot confirms that the reduced-order model obtained by parameter-varying projection indeed retains continuous dependence on the parameter. It further shows that the loci of the lightly damped modes in the reduced-order model almost exactly coincide with those of the original system. This is important, e.g., in order to perform flutter analyses on the reduced-order model.

C. Far Wakes of a Wind Turbine

As a second example, an unsteady aerodynamics problem known as the *actuator disk model* [38]–[40] is considered.

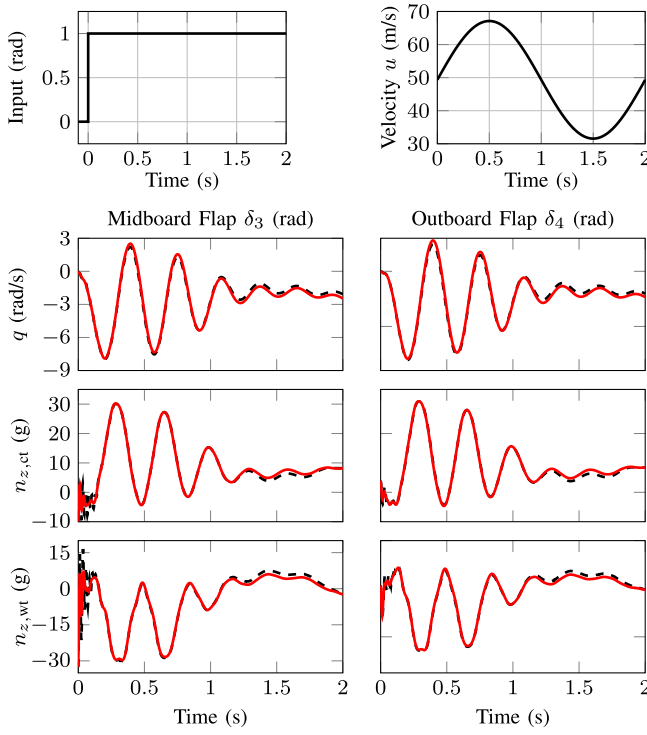


Fig. 5. X56A model: LPV Simulation of step response with varying parameter for full-order (--- 48 states) and reduced-order model (— 12 states).

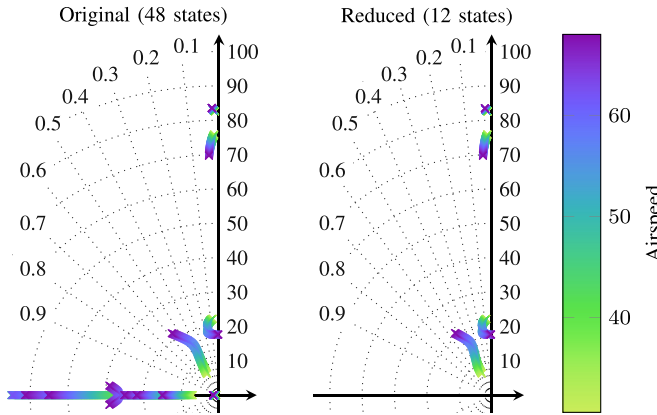


Fig. 6. X56A model: pole migration across flight envelope for full-order and reduced-order model.

It can be used to accurately model the far wake of a wind turbine by solving the 2-D Navier-Stokes equations for incompressible flows. The streamwise (x) and spanwise (y) velocity components are denoted by u and v and their dynamics are governed by the partial differential equations

$$\frac{\partial u}{\partial x} + \frac{\partial v}{\partial y} = 0 \quad (27a)$$

$$\frac{\partial u}{\partial t} + u \frac{\partial u}{\partial x} + v \frac{\partial u}{\partial y} = -\frac{1}{\rho} \frac{\partial P}{\partial x} + \nu \left(\frac{\partial^2 u}{\partial x^2} + \frac{\partial^2 u}{\partial y^2} \right) + f \quad (27b)$$

$$\frac{\partial v}{\partial t} + u \frac{\partial v}{\partial x} + v \frac{\partial v}{\partial y} = -\frac{1}{\rho} \frac{\partial P}{\partial y} + \nu \left(\frac{\partial^2 v}{\partial x^2} + \frac{\partial^2 v}{\partial y^2} \right) \quad (27c)$$

where ν is the kinematic viscosity and P is the pressure distribution. The forcing term f depends linearly on the thrust coefficient C_T of the turbine. This coefficient can be changed on a wind turbine via blade pitch or a change of the tip speed ratio and is thus a control input.

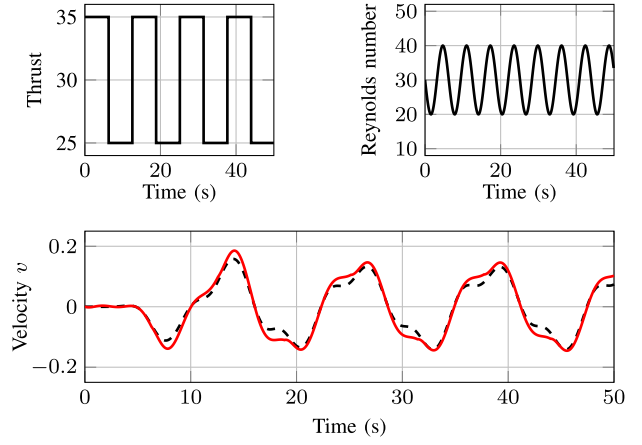


Fig. 7. Actuator disk model: Nonlinear simulation with fast varying parameter for full-order (--- 20502 states) and reduced-order model (— 6 states).

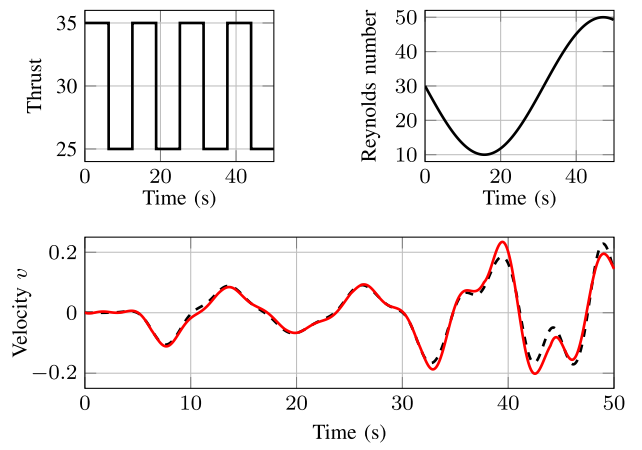


Fig. 8. Actuator disk model: Nonlinear simulation with slow varying parameter for full-order (--- 20502 states) and reduced-order model (— 6 states).

The particular configuration studied in this paper consists of two wind turbines, each with rotor diameter d , that are located $5d$ apart from each other in a 2-D stream of air. A prescribed inflow and a convective outflow condition are used, leading to the boundary conditions

$$\begin{aligned} u|_{x=0} &= U_\infty, \quad \frac{\partial u}{\partial t}|_{x=20d} + U_\infty \frac{\partial u}{\partial x}|_{x=20d} = 0 \\ v|_{x=0} &= 0, \quad \frac{\partial v}{\partial t}|_{x=20d} + U_\infty \frac{\partial v}{\partial x}|_{x=20d} = 0. \end{aligned} \quad (27d)$$

The upstream turbine runs with a constant thrust coefficient, while the downstream turbine's thrust coefficient is considered as a control input. The output is a measurement of the spanwise velocity component v , located $5d$ downstream from the second turbine, indicating far wakes. The partial differential equations are solved following standard computational fluid dynamics methods with a central difference scheme for spatial discretization. The grid is defined by 201 points in the streamwise direction and 51 points in the spanwise direction. The discretization yields an ordinary differential equation system with 20502 state variables that depends parametrically on the freestream velocity U_∞ , or in nondimensionalized form on the Reynolds number Re .

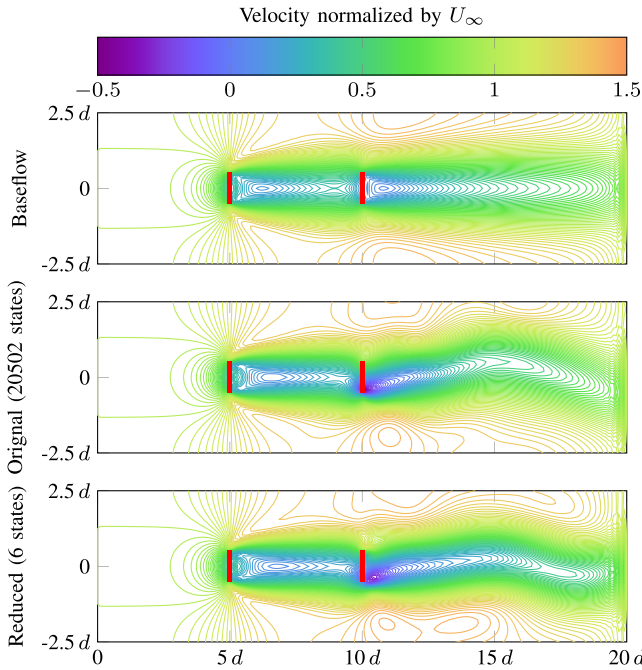


Fig. 9. Actuator disk model: Streamwise velocities u at $t = 40$ s corresponding to the simulation shown in Fig. 8 with locations of turbines (\cdot).

The system (27) is linearized for constant parameter values on the grid $Re = \{10, 20, 30, 40, 50\}$. Solving Lyapunov equations for the linearization of this large-scale system is intractable and hence empirical Gramians are used. They are obtained directly from sampling the simulated impulse response of the linearized system and its corresponding adjoint [18]. A forward Euler scheme and time steps of $t_s = 0.01$ s are used for time propagation with a time horizon of $t_N = 50$ s. The resulting trajectories are sampled every 0.5 s and result in empirical Cholesky factors at each grid point of size $20\,502 \times 100$. From these factors, a reduced-order model with six state variables is calculated. Simulation results for a sequence of step inputs and two different parameter trajectories are shown in Figs. 7 and 8. The responses of the reduced-order model are in excellent agreement with the full-order model. The speed of parameter variation appears to have no impact on the quality of the approximation, confirming that there is no neglected rate dependence in the reduction.

While the quality of the reduction should be strictly judged by how well the reduced-order system captures the considered input-output behavior, it remains insightful to look at the approximated state vector $x_{\text{approx}} = Vz$. For the considered problem, the original state vector has a clear physical interpretation, namely velocities in x and y direction at each of the 10251 nodes in the domain. Figs. 9 and 10 depict the baseflow that corresponds to a constant thrust coefficient $C_T = 30$ for both turbines and frozen-in-time snapshots taken from the simulation shown in Fig. 8. As expected, the reduced-order model is not able to completely resolve the full state accurately. Still, characteristic features of the stream are preserved up to the measurement point. The state variables of the reduced-order model can thus still be related to physically meaningful quantities. Velocities further downstream have

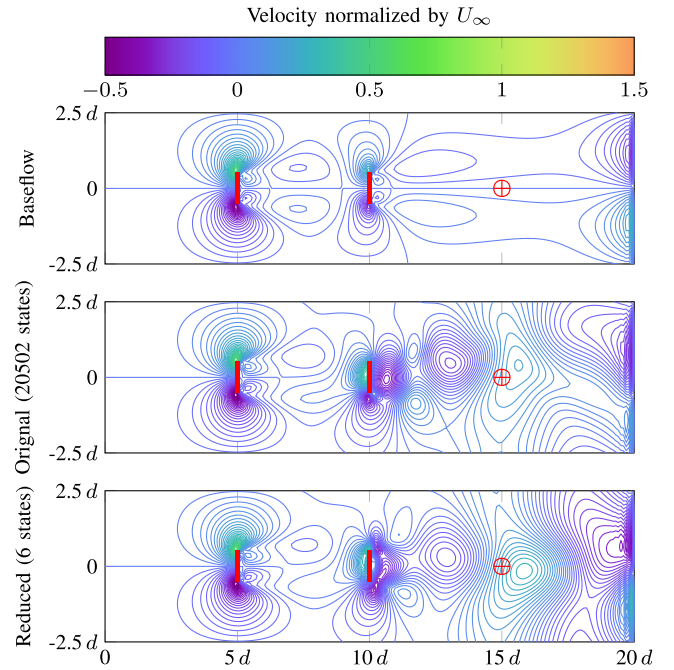


Fig. 10. Actuator disk model: Spanwise velocities v at $t = 40$ s corresponding to the simulation shown in Fig. 8 with locations of turbines (\cdot) and velocity measurement (\oplus).

little importance for the considered output and are hence less accurately resembled by the reduced-order model.

V. CONCLUSION AND EXTENSIONS

A model order reduction method for LPV systems is developed in this paper. The key technical contribution is a parameter-varying projection that maintains a well-defined LPV system with consistent state space basis across the parameter domain. This projection is partially parameter dependent, but, in contrast to general parameter-varying state space transformations, does not introduce additional rate dependence. It thus provides a middle ground between the potentially conservative use of constant transformations and the increase in complexity that comes with parameter dependent transformations. It is shown that the projection has an immediate application to approximate balanced truncation and related approaches that employ Gramians to quantify the importance of subspaces for model order reduction.

The proposed extension of the general projection framework to parameter-varying projections does not rely on a particular choice of basis and test spaces. Suitable subspaces for the projection can thus not only be calculated by the Gramian-based approach pursued in this paper, but also by entirely different means. For instance, moment matching with Krylov subspaces could be applied [7], [41].

It remains to investigate whether it is possible to relax the assumptions on observability and controllability to detectability and stabilizability. The properties may arise for some models obtained through discretizing partial differential equations. Further, sensitivity of the proposed method for systems that are stable but near instability remains to be addressed. Finally, many systems, particularly in the field

of aeroelastic systems, become unstable for some parameter values. The aircraft considered in Section IV-B, e.g., becomes unstable for larger airspeed. Model order reduction for unstable LPV systems remains a challenging open topic and adapting the method developed in this paper is ongoing work that also involves finding suitable alternatives for the quantification of the importance of a subspace.

ACKNOWLEDGMENT

The authors would like to thank B. Danowsky, C. Schulze, and T. Lieu for providing the X-56 model, as well as J. Annoni for providing the wind turbine model.

REFERENCES

- [1] F. Wu, X. H. Yang, A. Packard, and G. Becker, "Induced L_2 -norm control for LPV systems with bounded parameter variation rates," *Int. J. Robust Nonlinear Control*, vol. 6, nos. 9–10, pp. 2379–2383, Nov. 1996.
- [2] A. Hjartarson, A. Packard, and P. Seiler, "LPVTools: A toolbox for modeling, analysis, and synthesis of parameter varying control systems," *IFAC PapersOnLine*, vol. 48, no. 26, pp. 139–145, Dec. 2015.
- [3] G. D. Wood, "Control of parameter-dependent mechanical systems," Ph.D. dissertation, Dept. Mech. Eng., Univ. Cambridge, Cambridge, U.K., 1995.
- [4] G. D. Wood, P. J. Goddard, and K. Glover, "Approximation of linear parameter-varying systems," in *Proc. IEEE Conf. Decision Control*, vol. 1, Dec. 1996, pp. 406–411.
- [5] B. C. Moore, "Principal component analysis in linear systems: Controllability, observability, and model reduction," *IEEE Trans. Autom. Control*, vol. 26, no. 1, pp. 17–32, Feb. 1981.
- [6] D. Amsallem and C. Farhat, "An Online method for interpolating linear parametric reduced-order models," *SIAM J. Sci. Comput.*, vol. 33, no. 5, pp. 2169–2198, 2011.
- [7] C. Poussot-Vassal and C. Roos, "Generation of a reduced-order LPV/LFT model from a set of large-scale MIMO LTI flexible aircraft models," *Control Eng. Pract.*, vol. 20, no. 9, pp. 919–930, Sep. 2012.
- [8] F. D. Adegas, I. B. Sørensen, M. H. Hansen, and J. Stoustrup, "Reduced-order LPV model of flexible wind turbines from high fidelity aeroelastic codes," in *Proc. IEEE Int. Conf. Control Appl. (CCA)*, Aug. 2013, pp. 424–429.
- [9] J. Theis, B. Takarics, H. Pfifer, G. J. Balas, and H. Werner, "Modal matching for LPV model reduction of aeroservoelastic vehicles," in *Proc. AIAA SciTech*, 2015, pp. 1–12, paper 2015–1686.
- [10] Y. Wang, H. Song, K. Pant, M. J. Brenner, and P. Suh, "Model order reduction of aeroservoelastic model of flexible aircraft," in *Proc. AIAA SciTech*, 2016, pp. 1–13, paper 2016–1222.
- [11] P. Benner, S. Gugercin, and K. Willcox, (Aug. 2013). "A survey of model reduction methods for parametric systems," Max Planck Inst., Magdeburg, Germany, Tech. Rep. MPIMD/13-14. [Online]. Available: <http://www2.mpi-magdeburg.mpg.de/preprints/2013/14/>
- [12] U. Baur, C. Beattie, P. Benner, and S. Gugercin, "Interpolatory projection methods for parameterized model reduction," *SIAM J. Sci. Comput.*, vol. 33, no. 5, pp. 2489–2518, 2011.
- [13] H. Panzer, J. Mohring, R. Eid, and B. Lohmann, "Parametric model order reduction by matrix interpolation," *Automatisierungstechnik*, vol. 58, no. 8, pp. 475–484, Aug. 2010.
- [14] J. Theis, P. Seiler, and H. Werner, "Model order reduction by parameter-varying oblique projection," in *Proc. Amer. Control Conf.*, Jul. 2016, pp. 4586–4591.
- [15] F. Wu, "Control of linear parameter varying systems," Ph.D. dissertation, Dept. Mech. Eng., Univ. California, Berkeley, CA, USA, 1995.
- [16] C. de Villemagne and R. E. Skelton, "Model reductions using a projection formulation," *Int. J. Control*, vol. 46, no. 6, pp. 2141–2169, 1987.
- [17] Y. Saad, *Iterative Methods for Sparse Linear Systems*. Philadelphia, PA, USA: SIAM, 2000.
- [18] A. Antoulas, *Approximation of Large-Scale Dynamical Systems*. Philadelphia, PA, USA: SIAM, 2005.
- [19] A. J. Laub, M. T. Heath, C. Paige, and R. Ward, "Computation of system balancing transformations and other applications of simultaneous diagonalization algorithms," *IEEE Trans. Autom. Control*, vol. 32, no. 2, pp. 115–122, Feb. 1987.
- [20] A. Varga, "Balancing free square-root algorithm for computing singular perturbation approximations," in *Proc. IEEE Conf. Decision Control*, Dec. 1991, pp. 1062–1065.
- [21] D. F. Enns, "Model reduction with balanced realizations: An error bound and a frequency weighted generalization," in *Proc. IEEE Conf. Decision Control*, Dec. 1984, pp. 127–132.
- [22] G. Becker, A. Packard, D. Philbrick, and G. Balas, "Control of parametrically-dependent linear systems: A single quadratic Lyapunov approach," in *Proc. Amer. Control Conf.*, Jun. 1993, pp. 2795–2799.
- [23] S. Boyd and L. Vandenberghe, *Convex Optimization*. Cambridge, U.K.: Cambridge Univ. Press, 2004.
- [24] G. E. Dullerud and F. Paganini, *A Course in Robust Control Theory: A Convex Approach* (Texts in Applied Mathematics), vol. 36. New York, NY, USA: Springer, 2000.
- [25] G. J. Balas, "Linear, parameter-varying control and its application to a turbofan engine," *Int. J. Robust Nonlinear Control*, vol. 12, no. 9, pp. 763–796, Jul. 2002.
- [26] I. M. Jaimoukha and E. M. Kasenally, "Krylov subspace methods for solving large Lyapunov equations," *SIAM J. Numer. Anal.*, vol. 31, no. 1, pp. 227–251, 1994.
- [27] J.-R. Li and J. White, "Low rank solution of Lyapunov equations," *SIAM J. Matrix Anal. Appl.*, vol. 24, no. 1, pp. 260–280, 2002.
- [28] P. Benner, J.-R. Li, and T. Penzl, "Numerical solution of large-scale Lyapunov equations, Riccati equations, and linear-quadratic optimal control problems," *Numer. Linear Algebra Appl.*, vol. 15, no. 9, pp. 755–777, Nov. 2008.
- [29] K. Willcox and J. Peraire, "Balanced model reduction via the proper orthogonal decomposition," *AIAA J.*, vol. 40, no. 11, pp. 2323–2330, Nov. 2002.
- [30] S. Lall, J. E. Marsden, and S. Glavaški, "A subspace approach to balanced truncation for model reduction of nonlinear control systems," *Int. J. Robust Nonlinear Control*, vol. 12, no. 6, pp. 519–535, May 2002.
- [31] S. J. Hammarling, "Numerical solution of the stable, non-negative definite Lyapunov equation," *IMA J. Numer. Anal.*, vol. 2, no. 3, pp. 303–323, Jul. 1982.
- [32] R. Bartels and G. W. Stewart, "Solution of the matrix equation $AX + XB = C$ [F4]," *Commun. ACM*, vol. 15, no. 9, pp. 820–826, Sep. 1972.
- [33] G. H. Golub and C. F. Van Loan, *Matrix Computations*, 4th ed. Baltimore, MD, USA: The Johns Hopkins Univ. Press, 2013.
- [34] C. Desoer, "Slowly varying system $\dot{x} = A(t)x$," *IEEE Trans. Autom. Control*, vol. 14, no. 6, pp. 780–781, Dec. 1969.
- [35] J. Annoni, "Modeling for wind farm control," Ph.D. dissertation, Dept. Aeronaut. Eng. Mech., Univ. Minnesota, Minneapolis, MN, USA, 2016.
- [36] J. J. Ryan and J. T. Bosworth, "Current and future research in active control of lightweight, flexible structures using the X-56 aircraft," in *Proc. AIAA SciTech*, 2014, paper 2014-0597.
- [37] P. C. Schulze, B. P. Danowsky, and T. Lieu, "High fidelity aeroservoelastic model reduction methods," in *Proc. AIAA SciTech*, 2016.
- [38] J. N. Sørensen and A. Myken, "Unsteady actuator disc model for horizontal axis wind turbines," *J. Wind Eng. Ind. Aerodyn.*, vol. 39, nos. 1–3, pp. 139–149, 1992.
- [39] J. N. Sørensen and C. W. Kock, "A model for unsteady rotor aerodynamics," *J. Wind Eng. Ind. Aerodyn.*, vol. 58, no. 3, pp. 259–275, Dec. 1995.
- [40] J. R. Annoni, J. Nichols, and P. J. Seiler, "Wind farm modeling and control using dynamic mode decomposition," in *Proc. AIAA SciTech*, 2016, pp. 1–13.
- [41] S. Gugercin, "An iterative SVD-Krylov based method for model reduction of large-scale dynamical systems," in *Proc. IEEE Conf. Decision Control*, Dec. 2005, pp. 5905–5910.



Julian Theis received the bachelor's and master's degrees in mechanical engineering from the Hamburg University of Technology, Hamburg, Germany, in 2010 and 2013, respectively, where he is currently pursuing the Ph.D. degree.

He was a Visiting Scholar at the University of California, Berkeley, CA, USA, from 2011 to 2012, the German Aerospace Center DLR, Oberpfaffenhofen, Germany, from 2012 to 2013, and the University of Minnesota, Minneapolis, MN, USA, in 2014 and from 2015 to 2016. He is currently a Research

Assistant with the Hamburg University of Technology. His current research interests include robust and linear parameter-varying control, control-oriented model order reduction, and applications in the field of flight control and aeroservoelastic systems.



Peter Seiler received the Ph.D. degree from the University of California, Berkeley, CA, USA, in 2001.

From 2004 to 2008, he was with the Honeywell Research Labs, Minneapolis, MN, where he was involved in various aerospace and automotive applications including the redundancy management system for the Boeing 787, sensor fusion algorithms for automotive active safety systems, and re-entry flight control laws for NASA's Orion vehicle. He has been with the University of Minnesota, Minneapolis, MN, USA, since 2008. His current research interests include fault-detection methods for safety-critical systems and advanced control techniques for wind turbines and unmanned aircraft.



Herbert Werner received the Dipl.Ing. degree from Ruhr University, Bochum, Germany, in 1989, the M.Phil. degree from the University of Strathclyde, Glasgow, U.K., in 1991, and the Ph.D. degree from the Tokyo Institute of Technology, Tokyo, Japan, in 1995.

He was with the Control Engineering Laboratory, Ruhr University, from 1995 to 1998, and the Control Systems Center, University of Manchester Institute of Science and Technology, Manchester, U.K., from 1999 to 2002. He is currently the head of the Institute of Control Systems, Hamburg University of Technology, Hamburg, Germany. His current research interests include linear systems theory, robust and gain-scheduled control systems, networked control systems, and modeling of uncertain, nonlinear, and time-varying systems.